

## Candidate Source of Flux Noise in SQUIDS: Adsorbed Oxygen Molecules

Hui Wang,<sup>1,2</sup> Chuntai Shi,<sup>2,3</sup> Jun Hu,<sup>2</sup> Sungho Han,<sup>2</sup> Clare C. Yu,<sup>2</sup> and R. Q. Wu<sup>1,2,\*</sup>

<sup>1</sup>State Key Laboratory of Surface Physics and Department of Physics, Fudan University, Shanghai 200433, China

<sup>2</sup>Department of Physics and Astronomy, University of California, Irvine, California 92697-4575, USA

<sup>3</sup>Department of Physics, University of Wisconsin-Madison, Madison, Wisconsin 53706, USA

(Received 18 April 2015; published 14 August 2015; corrected 17 November 2015)

A major obstacle to using superconducting quantum interference devices (SQUIDS) as qubits is flux noise. We propose that the heretofore mysterious spins producing flux noise could be O<sub>2</sub> molecules adsorbed on the surface. Using density functional theory calculations, we find that an O<sub>2</sub> molecule adsorbed on an  $\alpha$ -alumina surface has a magnetic moment of  $\sim 1.8 \mu_B$ . The spin is oriented perpendicular to the axis of the O–O bond, the barrier to spin rotations is about 10 mK. Monte Carlo simulations of ferromagnetically coupled, anisotropic XY spins on a square lattice find  $1/f$  magnetization noise, consistent with flux noise in Al SQUIDS.

DOI: 10.1103/PhysRevLett.115.077002

PACS numbers: 85.25.Dq, 71.15.Mb, 73.50.Td, 74.25.Ha

Noise impairs the performance of a variety of devices based on superconducting circuits, e.g., photon detectors used in astrophysics [1], bolometers used in the search for dark matter [2], nanomechanical motion sensors [3], and quantum-limited parametric amplifiers [4]. Of particular interest are superconducting quantum interference devices (SQUIDS) [5] where low frequency  $1/f$  magnetic flux noise [6] is one of the dominant sources of noise in superconducting qubits [7–10]. Experiments indicate that flux noise is produced by a high density (of order  $5 \times 10^{17} \text{ m}^{-2}$ ) of fluctuating spins residing on the surface of normal metals [11] and superconductors [12,13], though it is independent of the materials [6]. Furthermore, experiments indicate that these spins are not independent, but rather may be clustered and have correlated fluctuations [14,15].

A number of models of flux noise have been proposed [13,16–19]. An early model of flux noise proposed that the spins are the magnetic moments of electrons in surface traps and that the spin orientation changes when an electron hops to a different trap [13]. Another model suggested that spin flips of paramagnetic dangling bonds occurred as a result of interactions with tunneling two-level systems [16]. Experimental indications of interactions between spins [12] led Faoro and Ioffe to suggest that flux noise is the result of spin diffusion via Ruderman-Kittel-Kasuya-Yosida (RKKY) interactions [17]. RKKY interactions between randomly placed spins produce spin glasses, and Monte Carlo simulations of Ising spin glass systems show that interacting spins produce  $1/f$  flux and inductance noise in agreement with experiment [18].

The microscopic origin of these spins remains unclear. Choi *et al.* [20] proposed that they are electrons in localized states at the metal-insulator interface, though spins have also been found on the surface of the dielectric, aluminum oxide, without a metal present [11]. Density functional theory (DFT) calculations [21] on sapphire ( $\alpha$ -Al<sub>2</sub>O<sub>3</sub>),

emulating the oxide layer that typically forms on surfaces of SQUIDS, indicate that thermodynamically stable charged vacancies are unlikely to be the source of flux noise because of the large energy differences associated with spin reorientation, though these energy differences decrease as the charge decreases. Lee *et al.* [21] used DFT to suggest that ambient molecules, such as OH, adsorbed on the surface could be the culprits, though the energy differences between different spin orientations is hundreds of degrees Kelvin, making thermal spin fluctuations unlikely.

Since SQUIDS are exposed to the atmosphere, we propose that the primary source of spins producing flux noise is O<sub>2</sub> molecules adsorbed on the surface. The free O<sub>2</sub> molecule has a spin triplet electronic configuration with a magnetic moment of  $2.0 \mu_B$  [22] and is strongly paramagnetic in its liquid phase. O<sub>2</sub> molecules adsorbed on metal or oxide surfaces can form ordered lattices and exhibit exotic magnetic properties [23]. A natural question is whether they retain a large magnetic moment on the surface of metal oxides as well as on the surface of dielectric materials used to encapsulate SQUIDS [24]. If they do retain a large moment, it is important to know the associated magnetic anisotropy energies (MAEs) that are the energy barriers for spin reorientation and hence key to understanding thermal fluctuations. Because of the weak spin-orbit coupling of oxygen, the MAEs of these systems are small, making them difficult to investigate theoretically and experimentally.

In this Letter, using systematic DFT calculations, we report that O<sub>2</sub> molecules with a surface density of  $1.08 \times 10^{18} \text{ m}^{-2}$  have a large magnetic moment,  $1.8 \mu_B/\text{molecule}$ , on an  $\alpha$ -Al<sub>2</sub>O<sub>3</sub> (0001) surface. These spin moments are weakly coupled and can reorient almost freely in a plane perpendicular to the O–O bond, with an energy barrier at the level of a few millikelvins. Our Monte Carlo simulations on ferromagnetically coupled, anisotropic XY spins

on a 2D square lattice suggest that they indeed produce  $1/f$  magnetization noise, and hence an  $O_2$  adlayer could be responsible for the flux noise found in SQUIDs. This would explain the long standing conundrum of why flux noise does not much depend on materials [6].

Our DFT calculations were performed with the Vienna *ab initio* simulation package (VASP) [25–28], using the Perdew–Burke–Ernzerhof functional [29] for the description of the exchange and correlation interactions among electrons. We treated  $O-2s2p$  and  $Al-3s3p$  shells as valence states and adopted the projector-augmented wave pseudopotentials to represent the ionic cores [30,31]. The energy cutoff of the plane-wave expansion was 500 eV. The spin-orbit coupling term was treated self-consistently using the noncollinear mode of VASP [32,33], and the magnetic anisotropy energy was determined through either the torque or the total energy method [34,35]. While our main results involved  $\alpha$ -alumina, some test calculations were also carried out for  $\gamma$ -alumina thin films and ultrathin alumina on a NiAl (110) surface to investigate the effects of surface roughness and complex morphology [36]. To mimic sapphire  $Al_2O_3$  (0001) surfaces, we constructed a periodic slab model; the repeating unit consists of 18 layers of atoms and a vacuum that is 15 Å thick along the surface normal. In the lateral plane, we used a  $2 \times 2$  supercell to dilute the adsorbates, corresponding to a surface density of  $1.08 \times 10^{18} \text{ m}^{-2}$ . The lattice constant in the lateral plane was fixed according to the optimized dimensions of bulk  $\alpha$ - $Al_2O_3$  ( $a = b = 4.81 \text{ Å}$ ,  $c = 13.12 \text{ Å}$ ). An  $11 \times 11 \times 1$  Monkhorst-Pack [37]  $k$ -point mesh was used to sample the Brillouin zone. The criteria for structural optimization are (1) the atomic force on each atom is less than  $0.01 \text{ eV/Å}$  and (2) the energy convergence is better than  $10^{-7} \text{ eV}$ .

To describe the strength of  $O_2$  adsorption, we define the binding energy per  $O_2$  molecule as

$$E_b = E_{O_2/Al_2O_3(0001)} - E_{Al_2O_3(0001)} - E_{O_2}, \quad (1)$$

where  $E_{O_2/Al_2O_3(0001)}$  and  $E_{Al_2O_3(0001)}$  are the total energies of the  $Al_2O_3$  slab with and without the  $O_2$  molecule on it.  $E_{O_2}$  is the total energy of the free  $O_2$  molecule in its gas phase. Through studies of various initial adsorption configurations, with the  $O_2$  molecule being placed on top of O, Al, and O–O bridge sites, we found that the most preferential absorption site for the  $O_2$  molecule is atop the Al site on the  $Al_2O_3$  (0001) surface, with a binding energy of  $-0.15 \text{ eV}$ . This indicates that the  $O_2$ - $Al_2O_3$  (0001) interaction is rather weak, which is understandable since the clean  $Al_2O_3$  (0001) surface is known to be inert towards adsorbates [38,39]. As shown by the red balls in Figs. 1(a) and 1(b), the absorbed  $O_2$  molecule is tilted by about 55 deg away from the surface normal. The optimized O–O bond length is 1.23 Å, which is close to the experimental value 1.21 Å [40]. The nearest O–Al distance is 2.17 Å, and the Al atom underneath is pulled up by about

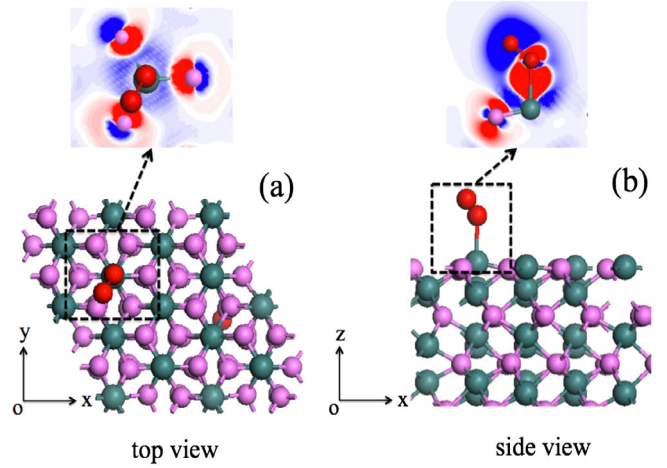


FIG. 1 (color online). Schematic atomic geometries of an  $O_2$  molecule absorbed on an  $Al_2O_3$  (0001) surface: (a) top view and (b) side view. The corresponding charge redistribution (the dashed rectangular area) between an adsorbed  $O_2$  molecule and the substrate is given in the insets: red and blue represent the charge accumulation and depletion at  $0.005 \text{ eV/Å}^3$ , respectively. The red balls and green balls represent the adsorbed  $O_2$  molecule and Al atoms, respectively. The magenta balls represent oxygen atoms in the  $Al_2O_3$  lattice.

$0.34 \text{ Å}$  from its position in the clean  $\alpha$ - $Al_2O_3$ (0001) surface, which is nevertheless still  $0.50 \text{ Å}$  lower than its bulklike position [41].

The total magnetic moment of each  $O_2$  molecule on  $Al_2O_3$  (0001) is  $1.8 \mu_B$ , slightly smaller than that in its gas phase,  $2.0 \mu_B$ . From the total density of states [peach background in Fig. 2(a)] and the projected density of states (PDOS) of the  $O_2$  molecule [blue and green peaks in Fig. 2(a)], it is also evident that the  $pp\pi^*$  orbitals of the  $O_2$  molecule in the minority spin channel split into two separate peaks and shift down to the Fermi level from 2.0 eV for the free  $O_2$  molecule. The small occupancy in the hybridized  $pp\pi^*$  orbitals causes the charge rearrangement as depicted in the insets of Figs. 1(a) and 1(b), and is responsible for the reduction of the magnetic moment of  $O_2$ . It appears that the lower oxygen atom in  $O_2$  and the lattice oxygen atoms gain electrons from Al and the higher oxygen atom in  $O_2$ . The spin density of the absorbed  $O_2$  molecule in the inset in Fig. 2(a) shows a donut feature of the  $pp\pi^*$  orbital, similar to that of the free  $O_2$  molecule. Meanwhile, the underlying Al and lattice O atoms are weakly magnetized, with small spin moments of 0.01 and  $0.03 \mu_B$ , respectively.

The two key parameters for  $1/f$  noise are the MAE and the exchange interaction between  $O_2$  molecules ( $J_{ij}$ ). Our DFT calculations with  $2 \times 2$  and  $4 \times 4$  supercells indicate  $O_2$  molecules interact ferromagnetically on  $Al_2O_3$  (0001), with exchange energies of 0.14 meV ( $\sim 1.6 \text{ K}$ ) for two oxygen molecules 4.8 Å apart, and 0.05 meV ( $\sim 0.6 \text{ K}$ ) for a separation of 9.6 Å. It appears that the substrate plays a

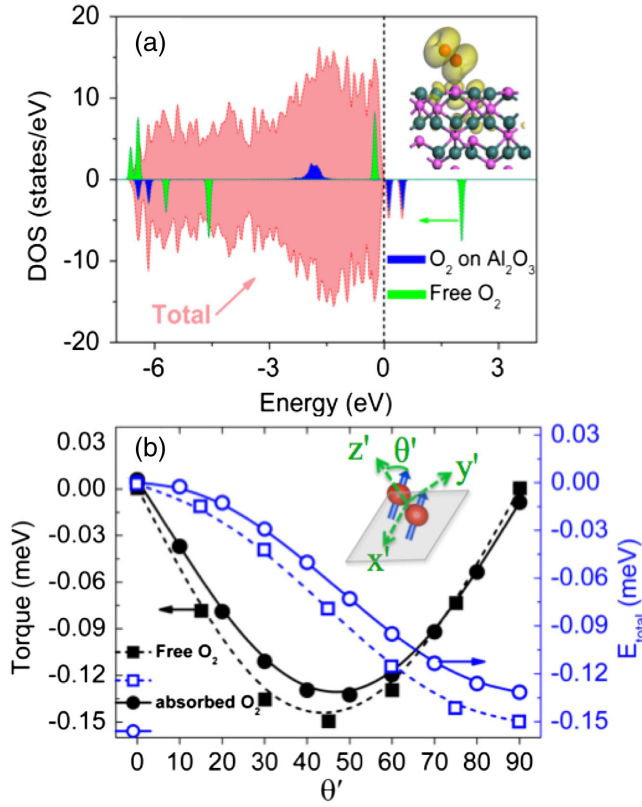


FIG. 2 (color online). (a) PDOS of the absorbed  $\text{O}_2$  molecule on  $\text{Al}_2\text{O}_3(0001)$ , along with the total density of states of  $\text{O}_2/\text{Al}_2\text{O}_3(0001)$  and the density of states of the free  $\text{O}_2$  molecule. The positive and negative values correspond to states in the majority and minority spin channels, respectively. The inset gives the isosurfaces (olive) of the total spin density of  $\text{O}_2/\text{Al}_2\text{O}_3(0001)$  at  $0.005 e/\text{\AA}^3$ . (b) Calculated torque and relative total energy ( $E_{\text{total}}$ ) versus the spin orientation of the free (dashed lines) and adsorbed (solid lines)  $\text{O}_2$  molecule. The inset defines the polar angle ( $\theta'$ ) for the direction of the spin with respect to the  $z'$  axis that lies along the O–O bond.

key role for the magnetic coupling between  $\text{O}_2$  molecules, because calculations for free  $\text{O}_2$  molecules gave smaller exchange values. As seen from the PDOS curves in Fig. S1 in the Supplemental Material [42], the  $pp\pi^*$  orbitals of antiferromagnetically coupled  $\text{O}_2/\text{Al}_2\text{O}_3(0001)$  shift to higher energies compared to their counterparts in ferromagnetically coupled  $\text{O}_2/\text{Al}_2\text{O}_3(0001)$ . This indicates a slightly smaller charge gain from Al when  $\text{O}_2$  spins are antiferromagnetically aligned compared to ferromagnetically aligned. Meanwhile, the induced spin polarization on the lattice oxygen atoms between two  $\text{O}_2$  molecules is also somewhat suppressed in the antiferromagnetic case. These factors favor ferromagnetic coupling between  $\text{O}_2$  molecules on  $\text{Al}_2\text{O}_3(0001)$ , as we will assume for the Monte Carlo simulations.

The determination of the small MAE of  $\text{O}_2$  is still a challenge for DFT calculations. We calculated the torque  $\tau(\theta')$  as a function of the polar angle  $\theta'$  of the spin moment with respect to the O–O bond that lies along the  $z'$  axis as

shown in the inset of Fig. 2(b):  $\tau(\theta') = [\partial E_{\text{total}}(\theta')/\partial\theta'] = \sum_{\text{occ}} \psi_{i,k} |(\partial H_{\text{SO}}/\partial\theta')| \psi_{i,k}$  [34,35], in steps of  $15^\circ$ , as illustrated in the inset. For the free  $\text{O}_2$  molecule,  $\tau$  follows the function  $-\sin(2\theta')$  as shown by the dashed black line in Fig. 2(b). By integrating  $\tau$  from 0 to  $\theta'$ , we obtain the angle dependence of the total energy,  $E_{\text{total}}(\theta')$ . Clearly, the lowest energy corresponds to the spin aligned perpendicular to the O–O bond ( $\theta' = 90^\circ$ ), and the energy difference between  $\theta' = 0^\circ$  and  $\theta' = 90^\circ$  is  $0.15 \text{ meV}/\text{O}_2$ . This stems from the spin-orbit coupling interaction between the  $pp\pi^*$  orbitals of  $\text{O}_2$  in the two separate spin channels, which are depicted by two sharp green peaks at  $-0.2 \text{ eV}$  (majority spin) and  $2.0 \text{ eV}$  (minority spin) in Fig. 2(a). Note that the spin rotation within the  $x'y'$  plane has no energy barrier for the free  $\text{O}_2$  molecule due to the cylindrical symmetry. Similarly, the torque associated with  $\text{O}_2/\text{Al}_2\text{O}_3$  also follows  $-\sin(2\theta')$  as shown by the solid black line in Fig. 2(b). The total energy decreases monotonically as the magnetic moment rotates away from the O–O bond towards the  $x'y'$  plane and the energy difference between  $\theta' = 0$  and  $\theta' = 90^\circ$  is  $0.13 \text{ meV}/\text{O}_2$ , slightly smaller than that of the free  $\text{O}_2$  molecule. This MAE is sufficient to block the thermal spin fluctuations out of the  $x'y'$  plane toward the  $z'$  axis at temperatures below 1 K. Nevertheless, spin can rotate within the  $x'y'$  plane, and the corresponding energy barrier is the key to determining its contribution to magnetic noise. By using the torque and total energy methods, we found that this energy barrier is extremely small [about  $1 \mu\text{eV}$  or  $10 \text{ mK}$ ], almost at the limit of the precision that DFT can achieve for the determination of the MAE, so rotation of spin within the  $x'y'$  plane is unblocked.

Knowing that the magnetic moments of  $\text{O}_2$  molecules are weakly coupled on  $\text{Al}_2\text{O}_3(0001)$  and can easily rotate around the O–O bond, we wanted to see if they produce the  $1/f$  noise observed in SQUIDs, rather than white noise (or a Lorentzian spectrum at low temperatures), so we performed Monte Carlo simulations of classical anisotropic XY spins. We focus on exchange interactions between oxygen spins since dipolar and hyperfine [19] interaction energies are much smaller, and describe the ferromagnetic nearest-neighbor exchange interactions with the Hamiltonian

$$H = -\sum_{\langle i,j \rangle} J_{ij} (S_i^x S_j^x + S_i^y S_j^y) - A \sum_i (S_i^x)^2, \quad (2)$$

where  $S_i^x$  is the  $x$  component of the spin on site  $i$  and  $A$  is the rescaled MAE. Without loss of generality, we choose the preferred anisotropic direction to be along the  $x$  axis, which we refer to as the “easy axis.” The length of the spins is 1. Since the SQUID surface is disordered and the oxygen molecules are adsorbed in random places, we choose ferromagnetic couplings  $J_{ij} > 0$  from a Poisson-like distribution  $P(J)$  in the following way. First, dimensionless integers  $C_{ij}$  are drawn from a Poisson distribution with a



mean of  $\langle C_{ij} \rangle = 5$ . Then,  $J_{ij} = 0.2J_0C_{ij}$ , where the average coupling  $\langle J_{ij} \rangle = J_0 = 1$  sets the energy and temperature scale. For  $A = 0$  and uniform coupling ( $J_{ij} = 1$ ), we obtain the traditional 2D XY model, which undergoes a Kosterlitz-Thouless phase transition [47] at  $T_C \sim 1$  (the exact value of  $T_C$  depends on the system size). We decided to use ferromagnetic couplings because (a) DFT finds ferromagnetic couplings, (b) the carrier density in the oxide is too low for spins to engage in RKKY interactions, and (c) there is experimental evidence for time reversal symmetry breaking consistent with surface spin ferromagnetism [14,18]. We performed Monte Carlo simulations with the Metropolis algorithm on a  $32 \times 32$  square lattice with periodic boundary conditions. In a trial move, a site and a trial angle between 0 and  $2\pi$  are randomly chosen from a uniform distribution. At each temperature, the system is allowed to equilibrate for  $10^6$  Monte Carlo steps per spin (MCS) before we record the time series for  $M(t)$ , the magnetization per spin, and for  $E(t)$ , the energy per spin. We then calculate the magnetization spectral density  $S_M(\omega) = 2 \int_{-\infty}^{\infty} dt e^{i\omega t} \langle \delta M(t) \delta M(0) \rangle$ , where  $\delta M(t) = [M(t) - \langle M \rangle]$ . We normalize the noise power by setting the total noise power equal to  $\sigma_M^2$ , the variance of  $M$ :  $S_{\text{tot}} = (1/N_\tau \sum_{\omega=0}^{\omega_{\text{max}}} S_M(\omega) = \sigma_M^2)$ , where  $N_\tau$  is the duration of the time series.

Our magnetization noise power results are shown in Figs. 3(a) and 3(b). At high frequencies  $S_M(f) \sim 1/f^\alpha$ , where the noise exponent  $\alpha$  varies from 0.3 to 2, depending on the temperature and anisotropy. At the Kosterlitz-Thouless transition ( $A = 0$  and  $T = T_C \sim 1$ ), our exponent is consistent with the expected value of

[48]  $\alpha = 1 + (2 - \eta)/z \sim 1.9$  with the critical exponent  $\eta = 1/4$  [49] and the dynamical critical exponent  $z \sim 2$  [50]. According to the actual values of  $J$  and  $A$  from the DFT calculations discussed above, the experimentally relevant parameters are  $T > 1.6$  and  $A \sim 0.01$ . In this regime, Figs. 3(c) and 3(d) show that the noise exponents range from 1.37 (for  $T = 1.6$ ) to 0.86 (for  $T = 2.0$ ), which is consistent with experimental values of 0.58 to 1 [6,9]. At low frequencies the noise is white due to a finite size effect [48]. We present additional results including the specific heat and susceptibility in the Supplemental Material [42].

It is now clear that the  $O_2$  molecules on qubits are magnetic and can produce  $1/f$  noise on  $Al_2O_3(0001)$ . Significantly, we found that the magnetic moment of  $O_2$  remains large and perpendicular to its bond as long as the molecule is not dissociated. Since most superconducting qubits have protective oxidized surfaces that are chemically inert, adsorbed  $O_2$  should remain in its molecular form. For example, physisorbed  $O_2$  molecules were found on Nb surfaces after the initial oxidation stages of the prototypical superconductor [51,52]. According to the mechanism discussed above for Al,  $O_2$  molecules should produce magnetic flux noise in these SQUIDS as well. Indeed, similar flux noise has been experimentally studied in SQUIDS fabricated from Al, Nb, Pb, and PbIn [6,7].

While vacancies on the oxide surfaces may also produce local magnetic moments, they contribute much less to the noise since, as we show in the Supplemental Material [42], the formation energy for both Al and O vacancies is high ( $>2.4$  eV) and hence their area density should be very low. Furthermore, none of the vacancies induces a magnetic moment on the more complex  $\gamma$ -alumina surface (see the Supplemental Material [42]). Our recent calculations have also found that the x-ray magnetic circular dichroism spectrum of an  $O_2$  adlayer has a sharp feature at the onset due to the transition from the  $1s$  shell to the characteristic  $2\pi^*$  orbitals of  $O_2$ , very different from that of O vacancies. This offers a useful way for experimental verification in the future. The identification of  $O_2$  adsorbates as the main source of magnetic noise has the important implication that one can reduce flux noise by protecting the surface with preoccupants such as  $NH_3$ ,  $N_2$ , or CO. Our preliminary results indicate that the adsorption energy of  $NH_3$  on sapphire is 1.8 eV per molecule, much higher than that of  $O_2$ , 0.15 eV.

In conclusion, systematic DFT calculations of  $O_2/Al_2O_3(0001)$  demonstrate that the physisorbed  $O_2$  molecule has a magnetic moment of  $\sim 1.8 \mu_B$  and a small magnetic anisotropy energy of 10 mK. Monte Carlo simulations of ferromagnetically coupled anisotropic XY spins on a square lattice find  $1/f$  magnetization noise, consistent with flux noise in Al SQUIDS. We thus propose that this could be the source of low frequency flux noise in SQUIDS. Unlike vacancies, which may or may not produce magnetic moments, depending on the charge state and their local environment [21], adsorbed  $O_2$  molecules have robust

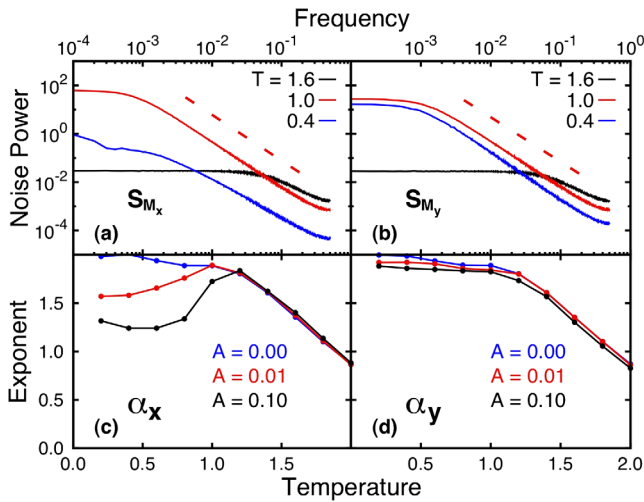


FIG. 3 (color online). (a),(b) Log-log plot of the magnetization noise power  $S_M(f)$  versus frequency (in units of  $0.1/\text{MCS}$ ) for (a)  $M_x$  and (b)  $M_y$ , at various temperatures for  $A = 0.01$ . The slopes of the dashed lines give the noise exponents  $\alpha$  and are (a) 1.89 and (b) 1.84 for  $T = 1$ . The noise spectra are taken from time series with  $10^7$  MCS and averaged over 50 sample realizations of the couplings. (c),(d) Noise exponents versus  $T$  for various values of the anisotropy for (c)  $M_x$  and (d)  $M_y$ .

magnetic moments because of their weak interaction with the substrate. Furthermore, the experimentally estimated density of fluctuating spins,  $5 \times 10^{17} \text{ m}^{-2}$  [11–13], is too high for vacancies, but is reasonable for the surface density of  $\text{O}_2$  adsorbates. Our results here imply that removing oxygen adsorbates from the surface of SQUIDs could substantially reduce flux noise.

We thank John Clarke and Robert McDermott for helpful discussions. Work at UCI was supported by DOE-BES (Grant No. DE-FG02-05ER46237) and the Army Research Office (Grant No. W911NF-10-1-0494). Work at Fudan was supported by the Chinese National Science Foundation under Grant No. 11474056. Computer simulations were performed at the U.S. Department of Energy Supercomputer Facility (NERSC).

\*To whom all correspondence should be addressed.

- [1] P. K. Day, H. G. LeDuc, B. A. Mazin, A. Vayonakis, and J. Zmuidzinas, *Nature (London)* **425**, 817 (2003).
- [2] *Cryogenic Particle Detection*, edited by C. Enss (Springer-Verlag, Berlin, 2005).
- [3] C. A. Regal, J. D. Teufel, and K. W. Lehnert, *Nat. Phys.* **4**, 555 (2008).
- [4] M. Hatridge, R. Vijay, D. H. Slichter, J. Clarke, and I. Siddiqi, *Phys. Rev. B* **83**, 134501 (2011).
- [5] J. Clarke and A. I. Braginski, *The SQUID Handbook* (Wiley-VCH, Weinheim, 2004).
- [6] F. C. Wellstood, C. Urbina, and J. Clarke, *Appl. Phys. Lett.* **50**, 772 (1987).
- [7] F. Yoshihara, K. Harrabi, A. O. Niskanen, Y. Nakamura, and J. S. Tsai, *Phys. Rev. Lett.* **97**, 167001 (2006).
- [8] K. Kakuyanagi, T. Meno, S. Saito, H. Nakano, K. Semba, H. Takayanagi, F. Deppe, and A. Shnirman, *Phys. Rev. Lett.* **98**, 047004 (2007).
- [9] R. C. Bialczak *et al.*, *Phys. Rev. Lett.* **99**, 187006 (2007).
- [10] J. Bylander, S. Gustavsson, F. Yan, F. Yoshihara, K. Harrabi, G. Fitch, D. G. Cory, Y. Nakamura, J.-S. Tsai, and W. D. Oliver, *Nat. Phys.* **7**, 565 (2011).
- [11] H. Bluhm, J. A. Bert, N. C. Koshnick, M. E. Huber, and K. A. Moler, *Phys. Rev. Lett.* **103**, 026805 (2009).
- [12] S. Sendelbach, D. Hover, A. Kittel, M. Mück, J. M. Martinis, and R. McDermott, *Phys. Rev. Lett.* **100**, 227006 (2008).
- [13] R. H. Koch, D. P. DiVincenzo, and J. Clarke, *Phys. Rev. Lett.* **98**, 267003 (2007).
- [14] S. Sendelbach, D. Hover, M. Muck, and R. McDermott, *Phys. Rev. Lett.* **103**, 117001 (2009).
- [15] S. M. Anton *et al.*, *Phys. Rev. Lett.* **110**, 147002 (2013).
- [16] R. de Sousa, *Phys. Rev. B* **76**, 245306 (2007).
- [17] L. Faoro and L. B. Ioffe, *Phys. Rev. Lett.* **100**, 227005 (2008).
- [18] Z. Chen and C. C. Yu, *Phys. Rev. Lett.* **104**, 247204 (2010).
- [19] J. Wu and C. C. Yu, *Phys. Rev. Lett.* **108**, 247001 (2012).
- [20] S. K. Choi, D.-H. Lee, S. G. Louie, and J. Clarke, *Phys. Rev. Lett.* **103**, 197001 (2009).
- [21] D. Lee, J. L. DuBois, and V. Lordi, *Phys. Rev. Lett.* **112**, 017001 (2014).
- [22] L. Pauling, *The Nature of the Chemical Bond and the Structure of Molecules and Crystals: An Introduction to Modern Structural Chemistry* (Cornell University Press, Ithaca, 1960), Vol. 18.
- [23] Y. Jiang, Y. Zhang, J. Cao, R. Wu, and W. Ho, *Science* **333**, 324 (2011).
- [24] A. Puglielli, S. Sendelbach, T. Klaus, and R. McDermott, *Bull. Am. Phys. Soc.* **58**, J36.13 (2013).
- [25] G. Kresse and J. Hafner, *Phys. Rev. B* **49**, 14251 (1994).
- [26] G. Kresse and J. Hafner, *Phys. Rev. B* **47**, 558 (1993).
- [27] G. Kresse and J. Furthmuller, *Phys. Rev. B* **54**, 11169 (1996).
- [28] G. Kresse and J. Furthmuller, *Comput. Mater. Sci.* **6**, 15 (1996).
- [29] J. P. Perdew, K. Burke, and M. Ernzerhof, *Phys. Rev. Lett.* **77**, 3865 (1996).
- [30] P. E. Blochl, *Phys. Rev. B* **50**, 17953 (1994).
- [31] G. Kresse and D. Joubert, *Phys. Rev. B* **59**, 1758 (1999).
- [32] D. Hobbs, G. Kresse, and J. Hafner, *Phys. Rev. B* **62**, 11556 (2000).
- [33] M. Marsman and J. Hafner, *Phys. Rev. B* **66**, 224409 (2002).
- [34] X. D. Wang, R. Q. Wu, D. S. Wang, and A. J. Freeman, *Phys. Rev. B* **54**, 61 (1996).
- [35] J. Hu and R. Wu, *Phys. Rev. Lett.* **110**, 097202 (2013).
- [36] G. Kresse, M. Schmid, E. Napetschnig, M. Shishkin, L. Kohler, and P. Varga, *Science* **308**, 1440 (2005).
- [37] H. J. Monkhorst and J. D. Pack, *Phys. Rev. B* **13**, 5188 (1976).
- [38] N. C. Hernández and J. F. Sanz, *J. Phys. Chem. B* **106**, 11495 (2002).
- [39] G. Zhao, J. Smith, J. Raynolds, and D. J. Srolovitz, *Interface Sci.* **3**, 289 (1996).
- [40] K.-P. Huber and G. Herzberg, *Constants of Diatomic Molecules* (Van Nostrand Reinhold New York, 1979), Vol. 4.
- [41] C. Verdozzi, P. A. Schultz, R. Q. Wu, A. H. Edwards, and N. Kioussis, *Phys. Rev. B* **66** (2002).
- [42] See Supplemental Material at <http://link.aps.org/supplemental/10.1103/PhysRevLett.115.077002>, for descriptions at DFT and Monte Carlo results on exchange couplings, the formation energies and effects of vacancies, and 2D interacting spin systems, which includes Refs. [43–46].
- [43] A. Kumar, J. Kumar, and S. Priya, *Appl. Phys. Lett.* **100**, 192404 (2012).
- [44] A. Sundaresan, R. Bhargavi, N. Rangarajan, U. Siddesh, and C. N. R. Rao, *Phys. Rev. B* **74**, 161306 (2006).
- [45] M. Venkatesan, C. B. Fitzgerald, and J. M. D. Coey, *Nature (London)* **430**, 630 (2004).
- [46] D. P. Landau and K. Binder, *A Guide to Monte Carlo Simulations in Statistical Physics* (Cambridge University Press, Cambridge, England, 2000).
- [47] J. M. Kosterlitz and D. J. Thouless, *J. Phys. C* **6**, 1181 (1973).
- [48] Z. Chen and C. C. Yu, *Phys. Rev. Lett.* **98**, 057204 (2007).
- [49] J. M. Kosterlitz, *J. Phys. C* **7**, 1046 (1974).
- [50] B. J. Kim, P. Minnhagen, S. K. Oh, and J. S. Chung, *Phys. Rev. B* **64**, 024406 (2001).
- [51] I. Lindau and W. E. Spicer, *J. Appl. Phys.* **45**, 3720 (1974).
- [52] R. Franchy, T. U. Bartke, and P. Gassmann, *Surf. Sci.* **366**, 60 (1996).